Subnormal Retinal Oxygenation Response Precedes Diabetic-like Retinopathy

Bruce A. Berkowitz,[1,2] *Renu A. Kowluru,*[3] *Robert N. Frank,*[2] *Timothy S. Kern,*[4] *Thomas C. Hohman,*[5] *and Manvi Prakash*[1]

Purpose. Determining which patients are at risk for the development of diabetic retinopathy is expected to greatly improve existing prevention and treatment options. In this study, using an animal model of diabetic retinopathy, the hypothesis was tested that magnetic resonance imaging (MRI) and a carbogen inhalation challenge provides important diagnostic information regarding the risk of developing diabetic retinopathy.

Methods. MRI was used to measure noninvasively the change in oxygen tension along the entire inner retina (i.e., from superior ora serrata to inferior ora serrata) during a carbogen (95% O_2/5% CO_2) inhalation challenge (IOVS 1996;37:2089). Two animal groups were examined by this MRI method at two time points: (1) rats fed either normal rat chow ($n = 20$) or a 50% galactose diet ($n = 20$) for 3.5 months (i.e., before the appearance of extensive retinal lesions) or (2) rats fed either normal rat chow ($n = 3$) for 15 months or a 30% galactose diet ($n = 4$) for 15 to 18 months (i.e., when lesions are present). Retinal biochemical and morphometric measurements were also obtained.

Results. After 3.5 months of galactosemia, before the appearance of extensive retinal morphologic lesions, a significant ($P < 0.05$) reduction in the panretinal oxygenation response was observed in the galactosemic group compared with its age-matched control. These galactose-fed animals also displayed a significantly ($P < 0.05$) larger oxygenation response in the inferior hemiretina than in the superior hemiretina. After 15 to 18 months of galactosemia, during the period when lesions are present, the panretinal oxygenation response remained significantly ($P < 0.05$) lower in the galactose-fed animals than in their age-matched controls. In contrast to the 3.5-month results, the oxygenation response in galactosemic animals at 15 to 18 months was significantly ($P < 0.05$) larger in the superior than in the inferior hemiretina. Hemiretinal oxygenation responses were not different in normal controls at either duration.

Conclusions. MRI measurement of the retinal oxygenation response to a carbogen challenge appears to be a powerful new and noninvasive approach that may be useful for assessing aspects of pathophysiology underlying the development of diabetic retinopathy in galactosemic rats. These results support our working hypothesis and suggest that further research into the diagnostic potential of this MRI approach for predicting the development of diabetic retinopathy is warranted. (*Invest Ophthalmol Vis Sci.* 1999;40:2100–2105)

Determining which patients are at risk for the development of diabetic retinopathy before retinal damage becomes clinically evident is expected to greatly improve existing prevention and treatment options.[1] It is commonly thought that early changes in retinal perfusion, perfusion reserve, and autoregulation are strongly associated with the subsequent appearance of diabetic retinopathy.[1,2] Consequently, rational management of diabetic retinopathy may be possible based on early detection of changes in retinal perfusion, perfusion reserve, and autoregulation.

To date, it has been difficult to accurately determine the magnitude and direction of early abnormalities in retinal perfusion, perfusion reserve, and autoregulation in diabetes.[1] Current noninvasive methods for measuring these physiological parameters are either not quantitative (e.g., fluorescein angiography), have limited spatial resolution and sensitivity (e.g., laser Doppler velocimetry), or are limited by media opacities such as cataracts (e.g., video fluorescein angiography). In experimental models, these noninvasive methods cannot be applied over long periods of time because of the relatively rapid formation of cataracts. Although invasive methods (e.g., microspheres[3]) have been used, such methods are highly destructive (which may confound data interpretation), suffer from limited sensitivity (e.g., few microspheres are captured) and limited spatial resolution (e.g., flow values represent the whole retina),

From the [1]Department of Anatomy and Cell Biology and [2]Kresge Eye Institute, Wayne State University, Detroit, Michigan; [3]Department of Ophthalmology and Visual Science, University of Wisconsin, Madison; [4]Department of Medicine/Endocrinology, Case Western Reserve University, Cleveland, Ohio; and [5]Wyeth–Ayerst Research, Princeton, New Jersey.

Supported by National Institutes of Health Grants RO1 EY10221 (BAB) and RO1 EY00300 (TSK), the Juvenile Diabetes Foundation International (RNF), and the American Diabetes Association (RAK).

Submitted for publication January 21, 1999; revised March 30, 1999; accepted April 29, 1999.

Proprietary interest category: N.

Reprint requests: Bruce A. Berkowitz, Department of Anatomy and Cell Biology, Wayne State University School of Medicine, 540 E. Canfield, Detroit, MI 48201.

and cannot be applied in humans. Clearly, there is a need for an accurate and sensitive measurement of retinal perfusion, perfusion reserve, and autoregulation that can be performed in the presence of cataracts.

In this study, a measure of retinal vascular perfusion, perfusion reserve, and autoregulation was achieved by determining the change in retinal oxygenation (ΔPo_2; units mm Hg) produced during a carbogen (95% O_2/5% CO_2) inhalation challenge (vide infra).[4–7] Normally, carbogen breathing induces a maximum oxygenation response from the retinal circulation.[4] However, if retinal perfusion or perfusion reserve are low, retinal autoregulation dysfunctional, or both, a smaller than normal ΔPo_2 will be produced during the carbogen challenge (vide infra).[7] The magnitude of the ΔPo_2 is noninvasively measured using magnetic resonance imaging (MRI). In earlier studies, we found good agreement between the MRI-measured ΔPo_2 and that determined using an oxygen electrode in normal rat retina under similar conditions.[4]

The purpose of this study is to begin testing the hypothesis that the retinal ΔPo_2, measured during a carbogen challenge, is strongly associated with the development of diabetic retinopathy. To this end, we measured the retinal ΔPo_2 before the appearance of extensive retinal lesions and during the period when retinal lesions were present in the galactose-fed rat model. The important features of the galactosemia model, in this context, are that it produces a diabetes-like retinopathy in 100% of the animals after more than 15 months, but without many of the metabolic anomalies associated with diabetes (e.g., alterations in the concentration of insulin, glucose, fatty acids, and amino acids).[8,9]

METHODS

The animals were treated in accordance with the National Institutes of Health *Guide for the Care and Use of Laboratory Animals* and the ARVO Statement on the Use of Animals in Ophthalmic and Vision Research.

Animal Model

The galactosemic rat model has been described in detail elsewhere.[10,11] Briefly, galactosemia was induced by feeding powered rat chow (Purina 5001) diluted with either 50% or 30% by weight with D-galactose for either 3.5 months ($n = 20$) or 15 to 18 months ($n = 4$), respectively. Age-matched controls ($n = 20$ or $n = 3$, respectively) were fed normal rat chow. The difference in galactose diets between the 3.5 and 15 to 18 month animals is not expected to confound data interpretation because the 30% and 50% galactose diets both result in essentially the same gross morphologic changes in the retinal vessels.[9] Animals scheduled for study were fasted overnight.

MRI Examination

On the day of the experiment, anesthesia was induced by a single intraperitoneal injection of urethane (36% solution, 0.083 ml/20 g animal weight, prepared fresh daily; Aldrich, Milwaukee, WI). Although a mild hyperglycemia is associated with urethane anesthesia,[12] the hyperglycemic response after the overnight fast did not differ ($P > 0.05$) among the groups. Each rat was gently positioned on an MRI-compatible homemade holder with its nose placed in a plastic nose cone. Animals were allowed to breathe spontaneously during the experiment. To maintain the core temperature of the rat, a recirculating heated water blanket was used. Rectal temperature, pulse, and hemoglobin oxygen saturation (data not shown) were continuously monitored while the animal was inside the magnet, as previously described.[4]

MRI data were acquired on a 4.7-T system using a two-turn transmit/receive surface coil (1.5 cm diameter) placed over the eye and an adiabatic spin–echo imaging sequence (repetition time [TR] 1 second; echo time [TE] 22.7 msec; number of acquisitions [NA] 1; matrix size, 128 × 256; slice thickness, 1 mm; field of view, 30 × 30 mm; sweep width, 25,000 Hz; 2 min/image). A capillary tube (1.5-mm inner diameter) filled with distilled water was used as the external standard. Five sequential 2-minute images were acquired as follows: four control images while the animal breathed room air and one image during carbogen breathing. Carbogen exposure was started at the end of the fourth image. Animals were returned to room air for 15 minutes to allow recovery from the inhalation challenge and removal from the magnet. Blood from the descending abdominal aorta was collected immediately after a second 2-minute carbogen challenge and analyzed for PaO_2, $PaCO_2$, pH, and glucose concentration. After the blood collection, the animal was euthanized with an intracardiac potassium chloride injection, and tissues were collected for further analysis (see below).

Attempts to measure preretinal vitreous Po_2 by subtracting images obtained during room air breathing and death (or hypoxemia) were not successful (data not shown). The major problem was that ocular perfusion pressure and eye shape changed from normal during death or hypoxemia. These changes significantly confounded quantitative pixel-by-pixel interpretation of the data. Furthermore, producing death or hypoxemia in humans is clearly problematic. Thus, we chose carbogen breathing because this method induces a maximum oxygenation response from the retinal circulation, makes detection of subtle differences between groups more robust and precise, and has clinical potential.

Data Analysis

To be included in this study, the animal must have demonstrated: minimal eye movement during the MRI examination, nongasping respiratory pattern before the MRI examination, rectal temperatures in the range 36.5°C to 38.5°C, and $PaO_2 >$ 350 mm Hg and $PaCO_2$ between 45 and 65 mm Hg during the carbogen challenge. The number of animals examined by MRI that satisfied the inclusion criterion for the 3.5-month control, 3.5-month galactosemia, 15- to 18-month control, and 15- to 18-month galactosemia groups were, respectively, 7, 10, 3, and 4. The MRI data from these animals were transferred to a Macintosh IIcx computer. Image registration was performed using software written inhouse for the program IMAGE (a freeware program available at http://rsb.info.nih.gov/nih-image/). After registration, the room air images were averaged to improve the signal–to–noise ratio. All pixel signal intensities in the average room air image and the 2-minute carbogen image were then normalized to the external standard intensity. On a pixel-by-pixel basis, signal intensity changes during carbogen breathing were calculated, converted to ΔPo_2 values, and displayed as a pseudocolor parameter map as previously described.[7] Data along a 1-pixel-thick line (200 μm) drawn in the preretinal vitreous space were extracted and displayed as a preretinal vitreous ΔPo_2 band. Each band represents ora ser-

Table 1. Summary of Blood Parameters Measured during a 2-Minute Carbogen Challenge

Blood Parameters	3.5-Month		15- to 18-Month	
	Control	Galactose-Fed	Control	Galactose-Fed
P_aO_2, mm Hg	597 ± 9	557 ± 22	536 ± 36	483 ± 81
P_aCO_2, mm Hg	50.6 ± 0.9	55.0 ± 1.0*	50.9 ± 1.9	51.6 ± 1.3
pH	7.32 ± 0.01	7.30 ± 0.01	7.30 ± 0.01	7.33 ± 0.00*
Glucose, mg/dl†	209 ± 12	171 ± 15	188 ± 5	244 ± 8

Values are mean ± SEM.
* $P < 0.05$, compared with age-matched controls.
† Elevated in all groups by the urethane anesthetic.

rata–to–ora serrata ΔPo_2 values over a 1-mm-thick section of retina (the MRI slice thickness). The width of the bands is arbitrary. The longer white tick mark in the center of each band represents the posterior pole near the optic nerve; the shorter tick marks represent 0.5-mm increments along the retinal surface.

Statistical Analysis

The physiological (i.e., blood gas values, rectal temperatures, and blood glucose data) and biochemical data were normally distributed and are presented as mean ± SEM. Comparisons were performed using an unpaired *t*-test, with $P < 0.05$ considered significant. The MRI and morphometric data were not normally distributed and are presented as the median. The nonparametric statistical tests used were as follows: a paired Wilcoxon signed ranked test using the individual oxygenation responses from each pixel in the region of interest to investigate superior–inferior hemiretinal differences within a group and a Kruskal–Wallis test. In all cases, $P < 0.05$ was considered significant. The individual oxygenation response bands for each animal in a group were combined on a pixel-by-pixel basis and displayed as a median band.

Biochemical Analysis

In the 3.5-month groups, retinal and blood samples were analyzed to determine the concentrations of glucose, galactose, galactitol, sorbitol, fructose, and myoinositol using methods previously described.[13] Retinal hexose and polyol concentrations were normalized to tissue protein levels. Red blood cell hexose and polyol concentrations were normalized to hemoglobin levels. The percent glycohemoglobin was measured using GlycoTestII affinity columns (Pierce, Rockford, IL). Note that the affinity columns do not differentiate between glucosylated and galactosylated hemoglobin. Samples were stored at −80°C for less than 3 weeks before the biochemical analyses.

Trypsin Digest

One half retina of one eye per animal was fixed in 10% buffered formalin. Trypsin digests of retinas from all groups were performed as previously described.[10] The digests were analyzed for acellular capillaries and pericyte ghosts in multiple fields across the entire sample and were expressed as the median frequencies of acellular capillaries per squared millimeter of retinal area and pericyte ghosts per 1000 capillary cells, respectively. Pericyte ghosts were defined as an "out pouching" of basement membrane on capillaries possessing at least one endothelia or pericyte nucleus. Because only four 15- to 18-month galactose-fed rats were available for this study, statistical statements concerning the retinal lesions in this group were not possible.

Results

Systemic Physiology

A summary of the blood parameters measured during a 2-minute carbogen challenge is present in Table 1. Although there were some differences between the galactose-fed and age-matched control groups, all the values fell within the expected range for carbogen breathing. The magnitude of the hyperglycemia associated with urethane[12] did not differ between the experimental groups.

Morphometric Analysis

The results of the morphometric analysis are presented in Table 2. The number of acellular capillaries was not statistically different ($P > 0.05$) between normal and galactosemic animals at 3.5 months and did not change ($P > 0.05$) with age in controls. No pericyte ghosts were found in either control group. The number of pericyte ghosts found in the galactose-fed animals at 3.5 months was small but statistically different from zero ($P < 0.05$). The number of long-term galactose-fed animals was not sufficient for statistical comparisons with age-matched control animals. Nonetheless, the trend in the data suggested that including more long-term galactosemic animals would have achieved statistical differences.

Retinal and Blood Biochemistry

Retinal and red blood cell levels of glucose, myoinositol, and fructose were not different ($P > 0.05$) between control and 3.5-month galactosemic rats (data not shown). Although the retinal concentrations of sorbitol were also not different ($P = 0.052$) between these two groups, red blood cell sorbitol levels were significantly ($P = 0.022$) lower in the galactose-fed animals. As expected, the 3.5-month galactosemic animals had significantly ($P < 0.05$) higher retinal concentrations of galactose (0.84 ± 0.06 nmol/mg, $n = 17$)) and galactitol (41.8 ± 6.8 nmol/mg, $n = 19$) compared with age-matched controls (undetectable). Similar biochemical data for the 15- to 18-month animals were not collected. However, such measurements have been previously reported for > 18-month galactosemic animals and are consistent with the present results.[13] Glyco-

TABLE 2. Summary of Morphometric Analysis

	3.5-Month		15- to 18-Month	
	Control	**Galactose-Fed**	**Control**	**Galactose-Fed**
Acellular capillaries, per min^2	1.2* (0–5.6)	2.3† (0–4.4)	3.2* (0–4)	7.5‡ (2.1–13)
Pericyte ghosts, per 1000 capillary cells	0* (0–0)	0.95† (0–1.5)	0* (0–4)	11.5‡ (5–16)

Values are median (range).

* $n = 7$ eyes from different animals. The data for animals for the 15- to 18-month control group were pooled from four 15- to 18-month animals not studied by MRI and three 15-month animals studied by MRI.

† $n = 8$ eyes from different animals.

‡ $n = 4$ eyes from different animals.

hemoglobin levels were significantly greater ($P < 0.05$) for the 3.5-month (7.1% ± 0.21%) and 15- to 18-month (6.1% ± 0.32%) galactosemic animals compared with their age-matched controls (1.4% ± 0.17% and 3.6% ± 0.22%, respectively).

MRI

In control eyes (Fig. 1, left), MRI provides a clear image of ocular anatomy including the retina/choroid complex (seen as a white line in the posterior region of the eye) and the nucleus and cortex of the lens. In the galactose-fed animals, the retina/choroid complex is also easily observed, even in the presence of a nearly complete cataract. The cataractous lens appears hyperintense in the 3.5-month galactose-fed rat (Fig. 1, right) and had a similar appearance in the 15- to 18-month galactosemic rats (not shown).

Figures 2 and 3 represent the median retinal oxygenation rate bands at 3.5 months and 15 to 18 months, respectively. Galactose feeding produced a significant ($P < 0.05$) reduction in panretinal oxygenation response before the appearance of extensive retinal vascular lesions (3.5 months of galactosemia, Fig. 2) and during the time when retinal vascular lesions were present (15–18 months of galactosemia, Fig. 3) compared with age-matched controls. Furthermore, at the 3.5-month time point, the largest oxygenation defect occurred in the superior hemiretina ($P < 0.05$). When the vascular lesions were apparent, the inferior hemiretina had the largest oxygenation defect ($P < 0.05$).

DISCUSSION

The results of the present study highlight the use of MRI and a carbogen inhalation challenge as a powerful quantitative and noninvasive approach that may be useful for assessing the risk of developing retinopathy. The measurement of retinal ΔPo_2 using MRI has several advantages: it is noninvasive; it is applicable to a wide range of age groups and species, possibly including humans; it can survey the entire two dimensional retinal surface; and it is not affected by media opacities, such as cataracts. Because early cataract formation occurs in many experimental diabetic animals, researchers using light-based methods must limit their measurement of retinal physiology to extremely early times (as short as 1 week in some studies) relative to the appearance of retinal lesions (over 1.5 years later). However, the relevance of such early information to the eventual appearance of retinal vascular lesions remains unclear. It is possible that such early changes may reflect only the short-term adaptations of the retinal circulation to the diabetic or galactosemic provocation and not the more likely relevant long-term changes induced by elevated blood sugar concentrations. These considerations underscore the application of MRI and a carbogen inhalation challenge as a new and potentially important diagnostic approach for assessing the risk for the development of diabetic retinopathy.

In the present study, we began to test our working hypothesis that a decrease in the retinal oxygenation response to a carbogen challenge is strongly associated with the development of diabetic retinopathy. Indeed, we found a significantly reduced panretinal oxygenation response in the galactose-fed rats both well before the appearance of extensive retinal lesions (at 3.5 months on the diet) and when lesions were evident (at 15–18 months on the diet). It is possible that the loss in retinal vasculature may contribute to the observed subnormal ΔPo_2 in the 15- to 18-month galactose-fed animals. However, this mechanism is not likely to play a role in the observed oxygenation response changes at 3.5 months (Table 2, vide infra). These data strongly support our working hypothesis and warrant further research into the diagnostic potential of our MRI approach in diabetic retinopathy.

Unexpectedly, we found an asymmetry in the hemiretinal oxygenation response before and after the appearance of ret-

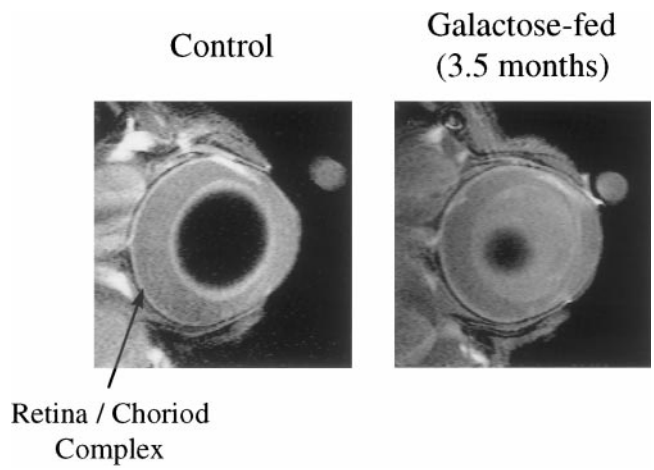

FIGURE 1. Representative MRI data (90 μm in plane resolution) from animals fed galactose for 3.5 months (*right*) and age-matched control animals (*left*). The *white line* in the posterior region of the eye represents the retina/choroid complex. Note that in the galactose-fed animals, the retina/choroid complex was easily observed, even in the presence of a nearly complete cataract (*right*). The *small circle* outside the eye is a water-filled capillary tube used as an external standard.

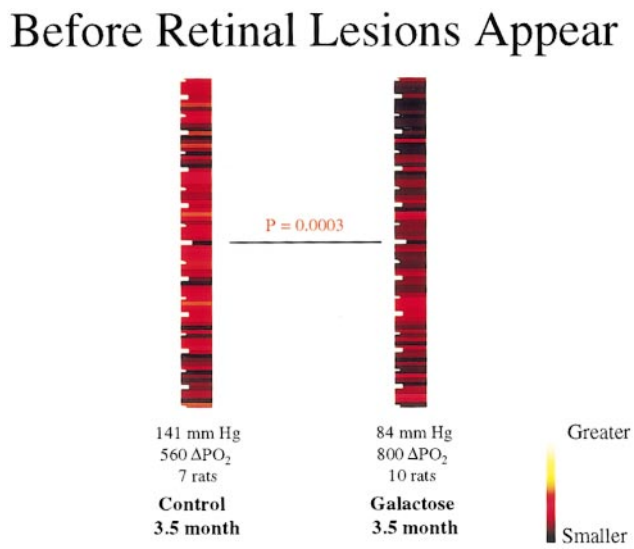

FIGURE 2. The median preretinal ΔPo_2 bands for the 3.5-month galactosemic and age-matched control groups. The same color scale was used for both groups. Pixels from the superior portion of the retina are at the top of the Figure. Note that the panretinal oxygenation response of the galactose-fed animals (median, 84 mm Hg; derived from 800 individual pixel ΔPo_2 values of 10 rats) is significantly lower ($P = 0.0003$) than that for the age-matched controls (median, 141 mm Hg; derived from 560 individual pixel ΔPo_2 values of 7 rats). Each band represents the pixel-by-pixel median ΔPo_2 value over a 1-mm-thick section of retina. (The displayed width of the bands is arbitrary.) The longer white tick mark in the center of each band represents the posterior pole near the optic nerve; the shorter tick marks represent 0.5-mm increments along the retinal surface.

inal lesions in the galactosemic groups. The superior hemiretinal ΔPo_2 in the 3.5-month galactosemic rats was significantly ($P < 0.05$) greater than the inferior ΔPo_2. This pattern was reversed in the 15- to 18-month galactosemic animals. The significance of these hemiretinal asymmetries is not clear and deserves further study.[14] The control group did not demonstrate a superior–inferior asymmetry at either time point. We are unaware of any reports describing a superior–inferior regional morphometric or physiological differences in experimental diabetic rat models.

The exact mechanisms underlying the reduction in panretinal oxygenation response in the galactosemic animals are not known. The following suggests that the subnormal ΔPo_2 is due to perturbations of retinal vascular physiology and not retinal oxygen consumption. The Po_2 of the posterior vitreous during room air breathing is a measure of the amount of oxygen supplied to the retina minus the amount consumed. During the carbogen challenge the amount of oxygen supplied to the retina increases approximately 400% (the arterial oxygen levels change from 100 to ≈500 mm Hg during the challenge). Because this increase is likely much greater than the change in retinal oxygen consumption, ΔPo_2 is expected to reflect primarily the change in retinal oxygen supply and to be sensitive to a variety of vascular physiological processes governing retinal oxygen supply during the carbogen challenge, such as retinal perfusion, perfusion reserve, and autoregulation.

Galactose-related biochemical alterations probably underlie the observed pathophysiology.[15] The subset of biochemical changes reported in this study is consistent with those in the literature.[13] However, establishing an association between these biochemical changes and the observed changes in retinal vascular physiology was beyond the scope of the present work. Nonetheless, MRI studies of the galactose model, and probably diabetic models, appear to be an appropriate system for future experiments designed to investigate the association between abnormal metabolism and pathophysiology.

The pathogenesis of diabetic retinopathy is unclear, although hypoxia may be responsible at least for its later-developing lesions, specifically neovascularization. Results of several studies in human and animal retinas indicate that vascular endothelial growth factor, a mitogen whose expression is known to be stimulated by hypoxia, appears in increased amounts in retinas of diabetic humans and animals that demonstrate few, or no, vascular lesions.[16,17] Direct experimental evidence supporting the hypoxia hypothesis has remained somewhat elusive.[18] Recent data from Linsenmeier et al. demonstrated an abnormally low preretinal vitreous Po_2 during room air breathing in long-term diabetic cats in the absence of gross retinal vascular morphology changes.[18] The low oxygenation response observed in the present study is also consistent with the presence of hypoxia, but it cannot yet be unambiguously interpreted as a measure of hypoxia. Experiments in this laboratory are ongoing to further study this relationship.

Acknowledgments

The oversight of the galactose rat model, and initial trypsin digests, by Alexander Kennedy is gratefully appreciated. We also thank Mark Larson and Linda Vandevelde for their technical assistance.

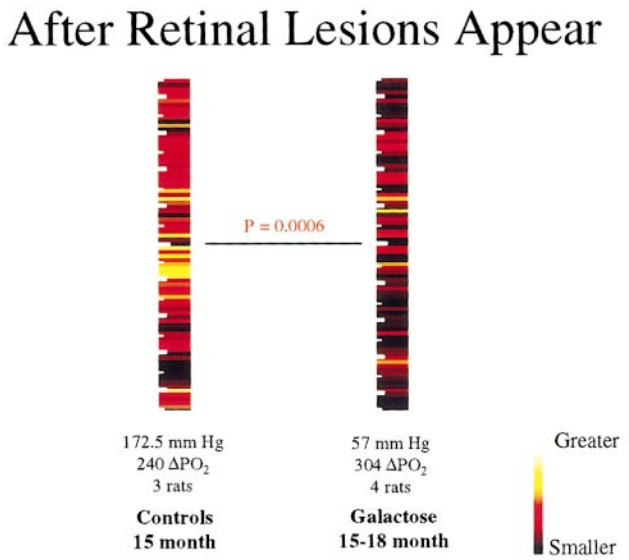

FIGURE 3. The median preretinal ΔPo_2 bands for the 15- to 18-month galactosemic and age-matched control groups. The color scale used in Figure 2 was also used for both groups in this Figure. Pixels from the superior portion of the retina are at the top of the Figure. Note that the panretinal oxygenation response of the galactose-fed animals (median, 57 mm Hg; derived from 304 individual pixel ΔPo_2 values of 4 rats) is significantly lower ($P = 0.0006$) than that for the age-matched controls (median, 172.5 mm Hg; derived from 240 individual pixel ΔPo_2 values of 3 rats). See legend of Figure 2 for more information.

References

1. Grunwald JE, Bursell S. Hemodynamic changes as early markers of diabetic retinopathy. *Curr Opinion Endo Diabetes.* 1996;3:298–306.
2. Harris A, Ciulla TA, Sung Chung H, et al. Regulation of retinal and optic nerve blood flow. *Arch Ophthalmol.* 1998;116:1491–1495.
3. Tilton RG, Weigel C, Eades D, et al. Increased ocular blood flow and 125 I-albumin permeation in galactose-fed rats: inhibition by sorbinil. *Invest Ophthalmol Vis Sci.* 1988;29:861–868.
4. Berkowitz BA. Adult and newborn rat inner retinal oxygenation during carbogen and 100% oxygen breathing. *Invest Ophthalmol Vis Sci.* 1996;37:2089–2098.
5. Berkowitz BA, Wilson CA. Quantitative mapping of ocular oxygenation using magnetic resonance imaging. *Magn Reson Med.* 1995; 33:579–581.
6. Berkowitz BA. Role of dissolved plasma oxygen in hyperoxia-induced contrast. *Magn Reson Imaging.* 1997;15:123–126.
7. Berkowitz BA, Penn JS. Abnormal panretinal response pattern to carbogen inhalation in experimental retinopathy of prematurity. *Invest Ophthalmol Vis Sci.* 1998;39:840–845.
8. Frank RN, Keirn RJ, Kennedy A, et al. Galactose-induced retinal capillary basement membrane thickening: prevention by sorbinil. *Invest Ophthalmol Vis Sci.* 1983;24:1519–1524.
9. Engerman RL, Kern TS. Retinopathy in animal models of diabetes. *Diabetes Metab Rev.* 1995;11:109–120.
10. Kern TS, Engerman RL. Galactose-induced retinal microangiopathy in rats. *Invest Ophthalmol Vis Sci.* 1995;36:490–496.
11. Robison WG Jr, Laver NM, Lou MF. The role of aldose reductase in diabetic retinopathy: prevention and intervention studies. *Prog Retinal Eye Res.* 1995;14:593–640.
12. Aisaka K, Kihara T, Koike M, et al. Effect of yohimbine on urethane-induced hyperglycemia in rats. *Jpn J Pharmacol.* 1989;49: 523–527.
13. Frank RN, Amin R, Kennedy A, et al. An aldose reductase inhibitor and aminoguanidine prevent vascular endothelial growth factor expression in rats with long-term galactosemia. *Arch Ophthalmol.* 1997;115:1036–1047.
14. Kern TS, Engerman RL. Vascular lesions in diabetes are distributed non-uniformly within the retina. *Exp Eye Res.* 1995;60:545–549.
15. Kowluru RA, Jirousek MR, Stramm LE, et al. Abnormalities of retinal metabolism in diabetes or experimental galactosemia. *Diabetes.* 1998;47:464–469.
16. Amin RH, Frank RN, Kennedy A, et al. Vascular endothelial growth factor is present in glial cells of the retina and optic nerve of human subjects with no proliferative diabetic retinopathy. *Invest Ophthalmol Vis Sci.* 1997;38:36–47.
17. Lutty GA, McLeod DS, Merges C, et al., Localization of vascular endothelial growth factor in human retina and choroid. *Arch Ophthalmol.* 1996;114:971–977.
18. Linsenmeier RA, Braun RD, McRipley MA, et al. Retinal hypoxia in long-term diabetic cats. *Invest Ophthalmol Vis Sci.* 1998;39:1647–1657.